Chemosphere 329 (2023) 138628

Contents lists available at ScienceDirect

Chemosphere

journal homepage: www.elsevier.com/locate/chemosphere

# Interactions between titanium dioxide nanoparticles and polyethylene microplastics: Adsorption kinetics, photocatalytic properties, and ecotoxicity

Gabriela Kalčíková [a,*], Rajdeep Roy [b], Barbara Klun [a], Ula Rozman [a], Gregor Marolt [a], Tina Skalar [a], Alexander Feckler [b,c], Mirco Bundschuh [b,d,**]

[a] Faculty of Chemistry and Chemical Technology, University of Ljubljana, Ljubljana, Slovenia
[b] iES Landau, Institute for Environmental Sciences, RPTU Kaiserslautern-Landau, Landau, Germany
[c] Eußerthal Ecosystem Research Station, RPTU Kaiserslautern-Landau, Eußerthal, Germany
[d] Department of Aquatic Sciences and Assessment, Swedish University of Agricultural Sciences, Uppsala, Sweden

## HIGHLIGHTS

- Titanium dioxide nanoparticles ($nTiO_2$) were rapidly adsorbed on microplastics (MPs).
- The experimental data fit well with the pseudo-second order kinetic model.
- Both suspended $nTiO_2$ and $nTiO_2$ immobilized on MPs were photocatalytic.
- Adsorption of $nTiO_2$ on MPs reduced the UV-induced toxicity of $nTiO_2$.

## GRAPHICAL ABSTRACT

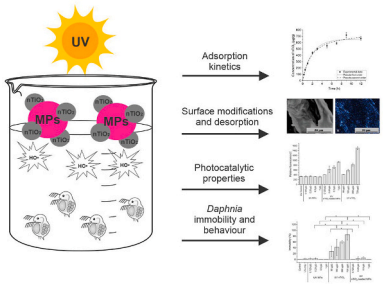


## ARTICLE INFO

Handling Editor: Michael Bank

*Keywords:*
Adsorption
Freshwaters
Microbeads
Nanoparticles
Reactive oxygen species

## ABSTRACT

The present study investigated the adsorption mechanism of titanium dioxide nanoparticles ($nTiO_2$) on polyethylene microplastics (MPs) and the resulting photocatalytic properties. This effort was supported by ecotoxicological assessments of MPs with adsorbed $nTiO_2$ on the immobility and behaviour of *Daphnia magna* in presence and absence of UV irradiation. The results showed that $nTiO_2$ were rapidly adsorbed on the surface of MPs (72% of $nTiO_2$ in 9 h). The experimental data fit well with the pseudo-second order kinetic model. Both suspended $nTiO_2$ and $nTiO_2$ immobilized on MPs exhibited comparable photocatalytic properties, with the latter showing a lower effect on *Daphnia* mobility. A likely explanation is that the suspended $nTiO_2$ acted as a homogeneous catalyst under UV irradiation and generated hydroxyl radicals throughout the test vessel, whereas the $nTiO_2$ adsorbed on MPs acted as a heterogeneous catalyst and generated hydroxyl radicals only locally and thus near the air-water interface. Consequently, *Daphnia*, which were hiding at the bottom of the test vessel, actively avoided exposure to hydroxyl radicals. These results suggest that the presence of MPs can modulate the phototoxicity of $nTiO_2$ – at least the location at which it is active – under the studied conditions.

* Corresponding author.
** Corresponding author. iES Landau, Institute for Environmental Sciences, RPTU Kaiserslautern-Landau, Landau, Germany.
*E-mail addresses:* gabriela.kalcikova@fkkt.uni-lj.si (G. Kalčíková), mirco.bundschuh@rptu.de (M. Bundschuh).

https://doi.org/10.1016/j.chemosphere.2023.138628
Received 13 February 2023; Received in revised form 3 April 2023; Accepted 5 April 2023
Available online 7 April 2023

## 1. Introduction

Plastic items of different types and sizes have been detected in water bodies worldwide with microplastics (MPs) being of significant scientific and societal interest (Rezania et al., 2018; Das et al., 2021). MPs are defined as plastic particles with a size between 1 and 1000 μm, and they can be further divided into primary and secondary MPs (Hartmann et al., 2019). Primary MPs are manufactured in a specific size, while secondary MPs are the result of fragmentation of larger plastic items (Hartmann et al., 2019). MPs can enter aquatic ecosystems from a variety of sources; one of the most important sources is urban dust, which contains secondary MPs derived from abrasion of road paint, car tyres, construction and building materials, and roadside litter (Horton et al., 2017; Patchaiyappan et al., 2021). Another important source is municipal wastewater, which mainly contains secondary MPs in the form of fibres (De Falco et al., 2019) and primary MPs from personal care products (often referred to as microbeads) (Napper et al., 2015; Godoy et al., 2019).

Regardless of the source, MPs can adsorb co-occurring pollutants as documented in freshwater and marine ecosystems (e.g. in Mai et al., 2018; Acosta-Coley et al., 2019). Indeed, numerous studies reported enhanced adsorption of various organic pollutants such as polychlorinated biphenyls (PCBs), polycyclic aromatic hydrocarbons (PAHs), perfluorinated alkyl substances (PFASs), polybrominated diethers (PBDs), pesticides, pharmaceuticals and personal care products (PPCPs) (Yu et al., 2019; Atugoda et al., 2021; Fu et al., 2021) and metal ions on MPs (Binda et al., 2021). Moreover, MPs may also interact with particulate stressors such as metal-based nanoparticles (NPs). For example, Li et al. (2020) investigated the adsorption of silver nanoparticles on polyethylene, polypropylene and polystyrene MPs. Moreover, Ferreira et al. (2016), Pacheco et al. (2018), and Davarpanah and Guilhermino (2019) focused on the combined ecotoxic effects of MPs (unknown polymer) and gold nanoparticles (co-exposure) on various aquatic organisms. However, the interactions between photoactive NPs and MPs have not been addressed to date, extending to the role of highly energetic light such as UV on their interactive effect. The latter may be of particular concern, as the presence of UV significantly enhances the ecotoxicity of photoactive NPs, such as $nTiO_2$ (Bundschuh et al., 2011; Kalčíková et al., 2014; Choi, 2016). Further relevance to address the interaction between MPs and $nTiO_2$ comes from their frequent use in personal care products (e.g., ZnO and $TiO_2$ NPs are used as inorganic UV filters and MPs as abrasives), inevitably leading to their joint presence in wastewaters as quantitatively confirmed elsewhere (Park et al., 2017; Liu et al., 2021). Moreover, if metal-based NPs are adsorbed on floating MPs (MPs made of low-density polymers) the exposure of NPs to sunlight, including UV is likely elevated. This higher UV exposure is particularly relevant for NPs with photoactive properties, such as $TiO_2$, and may lead to a higher production of reactive oxygen species (ROS), triggering ecotoxicological responses (Bundschuh et al., 2011; Feckler et al., 2015; Lüderwald et al., 2019).

Based on these assumptions, the present study targeted the interactions between low-density polyethylene (PE) MPs and $TiO_2$ NPs ($nTiO_2$). More specifically, we focused on the adsorption of $nTiO_2$ on MPs, the study of their photocatalytic properties under environmentally relevant UV intensities, and the evaluation of the individual and combined effects of MPs and $nTiO_2$ on the aquatic model organism (*Daphnia magna* Strauss, Cladoceran). It was hypothesized that (i) $nTiO_2$ can be well and stably adsorbed on the surface of MPs, and (ii) exhibits photocatalytic properties even after adsorption. In addition, it was assumed that (iii) the effect on *Daphnia* is reduced when $nTiO_2$ is adsorbed on MPs due to the limited bioavailability of $nTiO_2$ and the generated ROS.

## 2. Materials and methods

### 2.1. Microplastics and nanoparticles

MPs made of PE were extracted from a commercial facial scrub. MPs were separated by dissolving the cosmetic product in warm, deionized water. Subsequently, MPs were filtered through filter paper (pore size 4–12 μm), washed with deionized water, and dried at 60 °C (Kalčíková et al., 2017b). The MPs target concentration in each experiment was achieved by weighing them directly into each test vessel.

The $nTiO_2$ used in the present study were P25 obtained from Evonik (Germany). The stock suspension contained 2 g/L $nTiO_2$ in deionized water, which was pH stabilized (~3.3) by applying 120 μL/L of 2 M HCl. Before $nTiO_2$ were added to the test solution, the stock suspension was sonicated for 10 min to ensure homogeneous particle distribution and thus accurate transfer of particles into the test medium. The properties of used MPs and $nTiO_2$ are listed in Table 1.

The concentrations of MPs and $nTiO_2$ used in the adsorption, photocatalytic and ecotoxicity experiments are much higher than those found in the environment, which is motivated by the aim of the study that is providing a proof of principle. Moreover, these higher concentrations facilitate reliable analytical determination of, for example, metal content adsorbed on MPs or the monitoring of hydroxyl radicals.

### 2.2. Adsorption

#### 2.2.1. Adsorption kinetics

Experiments on adsorption kinetics were performed with 1 g/L MPs and 1 mg/L $nTiO_2$ in 100 mL synthetic freshwater medium (Borgmann, 1996) using 250-mL Erlenmeyer flasks on an orbital shaker (170 rpm) at 22 ± 2 °C for 48 h. For this experiment, 36 Erlenmeyer flasks were prepared. At each time point, i.e. 0, 0.25, 0.5, 1, 2, 3, 5, 7, 9, 12, 24, and 48 h, the entire content of three flasks were filtered through membrane filters (pore size 0.22 μm) and the filtrate was removed and stored at −18 ± 2 °C until further analysis. MPs that were retained on the filter were washed three times with 5 mL of deionized water. To determine the changes in the zeta potential of $nTiO_2$ during adsorption, three additional replicates were prepared and the zeta potential was measured over time using a Litesizer 500 (Anton-Paar GmbH, Austria).

The concentration of $nTiO_2$ adsorbed on MPs (abbreviated here as "$nTiO_2$-loaded MPs" in μg/g) as well as in the filtrate (μg/L) were determined. Briefly, the filtrate was diluted with 1% $HNO_3$ (1:1; *v:v*) and directly measured by an inductively coupled plasma optical emission spectrometer (ICP-OES) (Varian vista AX CCD Simultaneous ICP-OES, USA). $nTiO_2$-loaded MPs were dried at 40 °C to constant weight and transferred into a Teflon autoclave vessel. Afterwards, 7 mL of concentrated $HNO_3$ and 3 mL of concentrated $H_2SO_4$ were added. The autoclave vessels were heated to 220 °C for 20 min in a microwave digestion system (Ethos E, Milestone, Italy). After cooling, each sample was quantitatively transferred into a volumetric flask, filled up to 50 mL with ultrapure MilliQ water (resistivity >18.2 MΩ · cm), and measured by ICP-OES. Since $nTiO_2$ is used by the plastic industry as a white pigment and to increase UV resistance (Hahladakis et al., 2018; Luo et al., 2020), the initial content of titanium in MPs was also determined (< 1 μgTi/gMPs).

Two adsorption kinetic models were compared: the pseudo-first-order (Eq. (1)) and the pseudo-second-order model (Eq. (2)) (Lagergren, 1898; Ho and McKay, 1999; Sahoo and Prelot, 2020). These two models are often applied to reveal the rate-controlling step of the adsorption – if the data fit the pseudo-first order model better, adsorption rate is depended primarily of the adsorbate external and internal diffusion, while a better fit to the pseudo-second order model indicates that the binding of the adsorbate to the adsorbent is the rate controlling step (Wang and Guo, 2020).

$$q_t = q_e\left(1 - e^{-K_1 \cdot t}\right) \quad (1)$$

$$q_t = \frac{q_e^2 \cdot K_2 \cdot t}{1 + q_e \cdot K_2 \cdot t} \quad (2)$$

where, $K_1$ is the pseudo-first-order rate constant (1/h), $K_2$ is the pseudo-second-order rate constant (g/μg·h), $q_e$ is the amount of $nTiO_2$ adsorbed at equilibrium (μg/g), $q_t$ is the amount of $nTiO_2$ adsorbed at any time

(μg/g), and *t* is the time of adsorption (h).

#### 2.2.2. Desorption of $nTiO_2$ from MPs

A simple desorption study was performed to evaluate possible desorption (leaching) of $nTiO_2$ from $nTiO_2$-loaded MPs during further experiments. Three replicates of 1 g/L $nTiO_2$-loaded MPs in ASTM medium (a medium used in ecotoxicity tests (ASTM, 2007)) were prepared. The solution was left in darkness without stirring for 24 h to simulate the static condition of the ecotoxicity test. After the test, the concentration of $nTiO_2$ in ASTM was analysed (the description is given in the section 2.2.1).

#### 2.2.3. Surface analysis

Surface analysis of MPs and $nTiO_2$-loaded MPs (after the 48-h adsorption experiment; section 2.2.1) was done by field-emission scanning electron microscopy (FE-SEM, ULTRA plus, Zeiss, Germany). Therefore, the samples were fixed to aluminium stubs with carbon tape and coated with a thin Au/Pd layer (approximately 10 nm) before FE-SEM analysis. Image microscopy was performed at an accelerating voltage of 2 kV using an Evernhart-Thornley detector. A working distance of 5.5 mm between the final pole piece of the lens and the sample surface was used. The elemental composition of the samples was determined using energy dispersive X-ray spectroscopy (EDS). Elemental analysis in this study was performed using a silicon drift detector (SDD) (Oxford Instrument, UK) at an accelerating voltage of 20 kV to confirm the presence of $nTiO_2$ and later determine its distribution on the surface of MPs. Element maps were processed using Inca EDS acquisition program (Inca Suite version 4.15).

### 2.3. Photocatalytic properties

The photocatalytic properties of $nTiO_2$, and $nTiO_2$-loaded MPs were investigated according to the method described by Tang et al. (2005). Under UV irradiation, $nTiO_2$ generate hydroxyl radicals, which are then captured by sodium terephthalate. The obtained sodium 2-hydroxyterephthalate exhibits enhanced fluorescence intensity (Tang et al., 2005) and can therefore be used to monitor the photocatalytic activity of NPs (Feckler et al., 2015). Based on the results of the adsorption study (see section 3.1), the concentrations of $nTiO_2$ and MPs tested for their photocatalytic effects were 90, 180, 360, 720 μg/L and 0.125, 0.25, 0.5, 1 g/L, respectively. The concentrations of $nTiO_2$-loaded MPs were then set to 0.125, 0.25, 0.5, 1 g/L MPs with adsorbed 90, 180, 360, 720 μg $nTiO_2$, respectively. The suspension of $nTiO_2$, MPs and $nTiO_2$-loaded MPs was prepared in ASTM medium and each treatment was replicated three times. The photocatalytic properties were tested under visible light (800 − 1000 lx; OSRAM L 58W/21−840 ECO, Germany) and under UV light (Magic Sun 23/160 R 160W, Heraeus, Germany) in a temperature-controlled room (Weiss Environmental Technology Inc., Germany) at 20 ± 1 °C for 24 h. The intensities of UVA and UVB were 8.90 ± 0.97 $W/m^2$ and 0.45 ± 0.04 $W/m^2$ (mean ± SD; n = 20), respectively; measured at the water surface using a radiometer (RM12 radiometer; Dr. Gröbel UV-Elektronic GmbH, Germany). Those intensities are environmentally relevant as they are comparable to intensities measured on cloudy summer days in Germany (UVA = 6.5 $W/m^2$ and UVB = 0.3 $W/m^2$ in Kalčíková et al. (2014)). After 24 h (the incubation period was related to the duration of the ecotoxicity test; section 2.4), 8 mL of disodium terephthalate (1.3 g/L) was added into three replicates of each treatment that were located either under visible or UV light and allowed to react for 5 min (Tang et al., 2005). Then, three technical samples (300 μL) of each replicate were transferred to a 96-well microplate and the fluorescence was measured in a microplate reader (Tecan Infinite® M200, Tecan Group Ltd., Switzerland). The microplate reader used an excitation and emission wavelength of 310 and 430 nm, respectively, with the gain set to 121 (Lüderwald et al., 2019).

### 2.4. Ecotoxicity

Based on results of the adsorption study (see section 3.1) the concentrations of $nTiO_2$ and MPs tested for their ecotoxicological effects were 90, 180, 360, 720 μg/L and 0.125, 0.25, 0.5, 1 g/L, respectively. Concentrations of $nTiO_2$-loaded MPs were then set up to 0.125, 0.25, 0.5, 1 g/L MPs with adsorbed 90, 180, 360, 720 μg $nTiO_2$, respectively. All acute ecotoxicity tests were performed with *D. magna*, cultivated as described in Seitz et al. (2013), and largely followed the OECD Guideline 202 (OECD, 2004). Briefly, in the case of control, MPs and $nTiO_2$-loaded MPs, 100-mL beakers were filled with 50 mL ASTM medium and five juvenile *Daphnia* (age ≤ 24 h) were added. Afterwards, MPs or $nTiO_2$--loaded MPs were weighed directly into each replicate. In the case of $nTiO_2$, an appropriate volume of stock solution was pipetted into each replicate. The control and each concentration of MPs, $nTiO_2$, and $nTiO_2$-loaded MPs were replicated eight times, while four of these replicates were kept under visible light and thus in absence of UV light and the remaining four replicates were placed under UV light under the same conditions as described in section 2.3. After 12 and 24 h, the number of immobile *Daphnia* was counted. The experiment was repeated three times, while during the last two repetitions of the experiment, *Daphnia* from one replicate per treatment were additionally checked hourly for their location in the beaker (i.e. lower, middle or upper part). The observation was continued until the first immobile specimens were found (i.e., 11 observations per treatment were possible).

### 2.5. Statistics

Data on *Daphnia* immobility were compared between corresponding concentrations of $nTiO_2$ or MPs, therefore comparing UV MPs, UV $nTiO_2$ and UV $nTiO_2$-loaded MPs treatments. The normality and homogeneity of variances were tested with Shapiro-Wilk test and Levene's test, respectively. As the data were not normally distributed, the Kruskal-Wallis test was used, following the Dunn's post hoc test. For comparison between control or UV only and different treatments, the Mann-Whitney *U* test was used. Differences were considered statistically significant if $p < 0.05$. All data analyses were performed using OriginPro 2022b software (OriginLab Corp., USA).

For the analysis of *Daphnia* location in the test vessels, the ratio of organisms in the upper two sections of the test beaker to those organisms at the bottom section was abstracted. Based on these ratios, the distribution of *Daphnia* was categorized into "UP" (5 organisms in upper and middle section: 0 organisms in bottom section and 4:1), "EQUAL" (3:2 and 2:3), and "DOWN" (1:4 and 0:5). With this categorial response variable, a multinomial logistic regression model (function multinom in the R package nnet (Venables and Ripley, 2002)) including the interaction between the predictors "TREATMENT" and "UV" was fitted, while the distribution "UP" was set as the reference. Afterwards, a stepwise model selection was run based on Bayesian Information Criterion reduction to remove predictors that are not relevant for the model or have low explanatory power. Finally, the Wald test was applied on the best fitting model to examine the statistical significance of the estimated

**Table 1**
Properties of microplastics (MPs) and nanoparticles ($nTiO_2$) used in this study.

| | Material | Specific surface area ($cm^2/g$) | Number of particles per mg | Zeta potential (mV) | Mean particle size | Reference |
|---|---|---|---|---|---|---|
| MPs | Polyethylene | 62 | 96 | / | 148 μm | Rozman et al. (2021) |
| $nTiO_2$ | 70% anatase and 30% rutile | 50 000 | / | −10.79* | 21 nm | Lüderwald et al. (2019) |

Note: / – Not determined, * – Zeta potential of 4 mg/L $nTiO_2$ in ASTM medium.

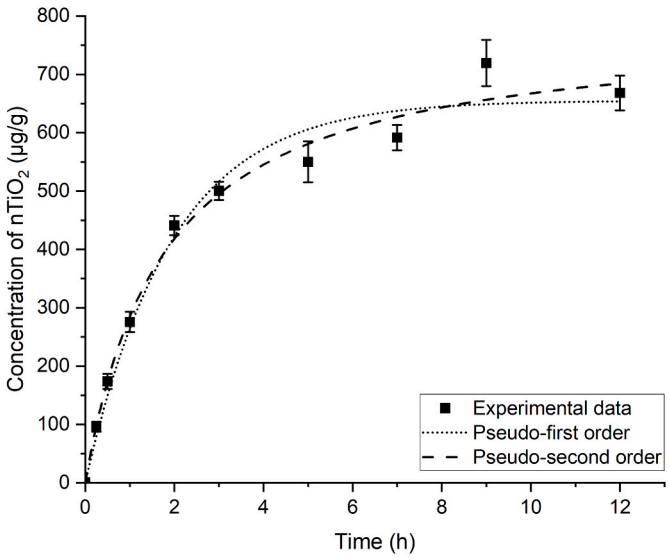


**Fig. 1.** Experimental data of adsorption process during the first 12 h (mean ± SD; n = 3) and fitted pseudo-first and pseudo-second order models to the experimental data.

coefficients. Data analyses were conducted using the open source software R (R Core Team, 2020) supplemented by the required add-on packages.

## 3. Results

### 3.1. Adsorption study

Most of the $nTiO_2$ was adsorbed on MPs surface in the first 9 h (72%, Fig. 1). The equilibrium concentration of $nTiO_2$ was 720 ± 40 µg/g and the remaining concentration of $nTiO_2$ in the solution was 310 ± 2 µg/L. The zeta potential did not change with time and was on average −14.1 ± 1.6 mV. The desorption experiment showed a good stability of adsorbed $nTiO_2$ on MPs, because after 24 h the concentrations of $nTiO_2$ in ASTM were still below the detection limit (< 1 µg/L).

The comparison of the two kinetic models showed relatively good fits of both models ($R^2$ was 0.9787 and 0.9874 for pseudo-first and pseudo-second order, respectively), however, comparison of calculated and experimental values of $q_e$ indicated a better fit of the pseudo-second order model (Table 2).

The adsorbed $nTiO_2$ on MPs surface (MPs surface; Fig. 2A) was visualized by FE-SEM showing an almost uniform distribution of $nTiO_2$ (Fig. 2B). But from the elemental map (Fig. 2C and D), it is evident that increased titanium concentrations, and thus $nTiO_2$, are found at certain locations, which is due to the structurally complex surface of MPs.

### 3.2. Photocatalytic properties

In the absence of UV light, the relative fluorescence units were ~300 for all treatments (data not shown). This is comparable to the levels measured in the sole presence of UV light and MPs (UV only and UV MPs in Fig. 3). This suggests that UV light alone and its combination with MPs does not produce hydroxyl radicals. Contrary, UV light in combination with $nTiO_2$ and $nTiO_2$-loaded MPs caused a concentration-dependent increase in relative fluorescence confirming the formation of hydroxyl radicals with increasing concentration (Fig. 3). Concentrations of 180 µg/L and 0.25 g/L of $nTiO_2$ and $nTiO_2$-loaded MPs, respectively, were the lowest concentrations at which a statistically significant difference was observed compared to the control. Although the concentrations of $nTiO_2$ in the treatments with MPs were the same as those concentrations in the $nTiO_2$ only treatment, the relative fluorescence was notably higher in the 720 µg/L $nTiO_2$.

### 3.3. Ecotoxicity

The immobility of *Daphnia* was at 0% in all treatments (i.e. control, MPs, $nTiO_2$-loaded MPs, and $nTiO_2$) during the entire duration of the experiment (i.e. 24 h) in the absence of UV light (data not shown).

In the presence of UV light, however, the immobility of *Daphnia* reached up to 10% after 12 h of exposure in all treatments except those only containing $nTiO_2$ (Fig. 4A). In the latter treatments, immobility was substantially higher, namely up to 85% (mean ± SD; n = 3). The statistical tests supported the descriptive statistics pointing towards significant difference only in presence of $nTiO_2$ (Table S1). After 24 h, immobility of *Daphnia* increased in all treatments including the UV-only treatment (in absence of MPs or $nTiO_2$, Fig. 4B). With increasing concentrations of $nTiO_2$-loaded MPs and MPs, a slight trend toward a decrease in immobility was observed. The decrease in immobility was at the highest concentration of $nTiO_2$-loaded MPs (1 g/L) statistically significantly different compared to corresponding $nTiO_2$ treatment (720 µg/L).

In the absence of UV light, *Daphnia* were uniformly located in each part of the beaker (Fig. 5A) while under UV, *Daphnia* were preferentially located at the bottom of the beaker and rarely in the upper part (Fig. 5B). Statistics confirmed that the presence of UV light was the only parameter that had a statistically significant effect ($p < 0.001$) on the location of *Daphnia*.

## 4. Discussion

Both MPs and NPs receive significant public attention due to their potential risks for the environment and human health (Burns and Boxall, 2018; Malakar et al., 2021). Numerous studies have investigated the fate and effects of MPs or NPs in aquatic systems (e.g. reviewed in Ma et al. (2020) and Cypriyana et al. (2021), respectively), while a limited number of studies have focused on their interactions (but see e.g., Li et al. (2020) and Ferreira et al. (2016)). In the present study, the adsorption of $nTiO_2$ on MPs and subsequent implications were investigated. $nTiO_2$ were rapidly adsorbed on MPs and evenly distributed on their surface (Fig. 2). The rate of adsorption process on microplastics is usually controlled by external diffusion (i.e., diffusion through the boundary layer) or binding process of the adsorbate on adsorbent (Wang and Guo, 2020). The good fit to the pseudo-second order model indicated that the adsorption rate is controlled by the binding of the $nTiO_2$ on the MPs surface and the rate of the adsorption mostly depends on the concentration of the MPs and $nTiO_2$ (Sahoo and Prelot, 2020; Wang and Guo, 2020). The rate constant $K_2$ was relatively small, but similar to the

**Table 2**
Parameters for the pseudo-first order model and the pseudo-second order model for $nTiO_2$ adsorption on MPs.

| | | Pseudo-first-order model | | | Pseudo-second-order model | |
|---|---|---|---|---|---|---|
| $q_{e\ exp}$ (µg/g) | $K_1$ (1/h) | $R^2$ (/) | $q_{e\ cal}$ (µg/g) | $K_2$ (g/µg·h) | $R^2$ (/) | $q_{e\ cal}$ (µg/g) |
| 720 | 0.517 | 0.9787 | 645 | 0.00073 | 0.9874 | 784 |

Note: $q_{e\ exp}$ – Experimental $nTiO_2$ concentration at equilibrium, $q_{e\ cal}$ – Calculated $nTiO_2$ concentration at equilibrium, $R^2$ – Correlation coefficient, $K_1$ – Pseudo-first order rate constant, $K_2$ – Pseudo-second order rate constant.

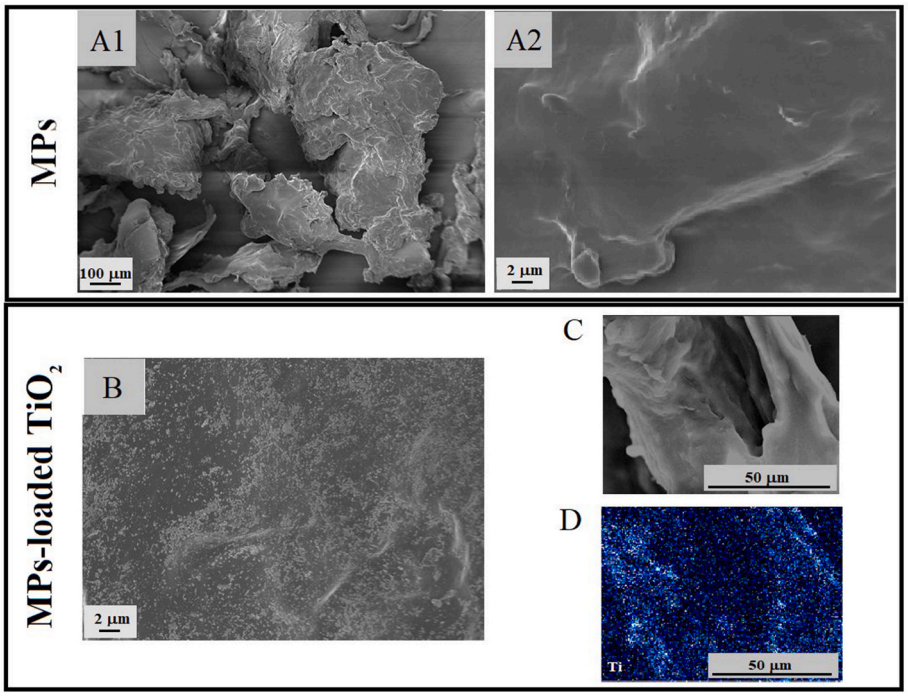


**Fig. 2.** FE-SEM images show A1 and A2) the surface of MPs, B) the surface of $nTiO_2$-loaded MPs where white spots are adsorbed $nTiO_2$, C) $nTiO_2$-loaded MPs and D) the element map of titanium on the corresponding MP particle displayed in (C).

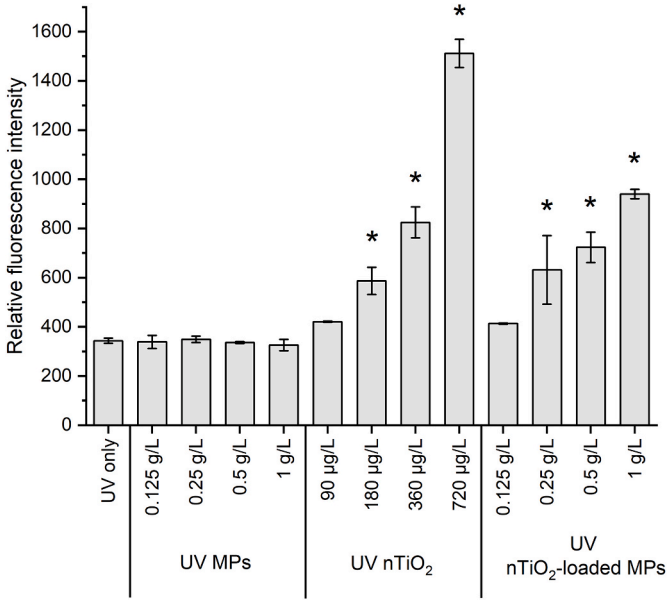


**Fig. 3.** Relative fluorescence intensity (mean ± SD; n = 3) – serving as proxy for hydroxyl radicals – in the sole presence of UV light (= UV only) and when UV light is combined with MPs (c = 0.125, 0.25, 0.5, 1 g/L), $nTiO_2$ (c = 90, 180, 360, 720 µg/L), and $nTiO_2$-loaded MPs (c = 0.125, 0.25, 0.5, 1 g/L with adsorbed 90, 180, 360, 720 µg $nTiO_2$, respectively) after 24 h. Asterisks denote significant differences in the relative fluorescence compared to the UV treatment (without MPs or $nTiO_2$).

study by Li et al. (2020), where the rate constant for the adsorption of silver nanoparticles on PS MPs was 0.0005 g/(µg·h).

It is likely that the initial interactions between MPs and $nTiO_2$ are of electrostatic nature, as the two particles carry opposite charges attracting each other. $nTiO_2$ had a negative charge (Table 1) due to Ti–OH and $Ti–O^-$ surface groups, which dominate (over $Ti–OH_2^+$) at neutral and alkaline conditions ((Chibowski and Paszkiewicz, 2001) (the pH of ASTM medium was 7.8)), while PE MPs most likely carried a positive charge (Kalčíková et al., 2017a). In addition, Cai et al. (2019) investigated the interactions between $nTiO_2$ and PS MPs and suggested that the presence of both positive and negative charged $nTiO_2$ may decrease MPs transport in porous media (i.e. quartz sand) and thus alter the fate of MPs in the environment. It is evident that the interactions between MPs and NPs are very complex and they depend on many factors, such as the type and size of MPs and NPs, ionic strength, and the pH of the medium, as well as the presence of natural organic matter (Li et al., 2020; Cao et al., 2021). Given the complexity of realistic environmental conditions, the detailed investigation of their interactions requires more attention and additional studies.

The results of the photocatalytic experiment showed that, under UV radiation, both suspended $nTiO_2$ and $nTiO_2$ adsorbed on MPs ($nTiO_2$-loaded MPs) had photocatalytic properties (Fig. 3) and catalysed the decomposition of $H_2O$ into hydroxyl radicals (Zhang and Nosaka, 2014). Since the desorption of $nTiO_2$ from the surface of MPs into the medium was negligible, it is expected that hydroxyl radicals were generated by suspended $nTiO_2$ and immobilized $nTiO_2$ ($nTiO_2$-loaded MPs) in different ways, i.e., by homogeneous and heterogeneous photocatalysis, respectively (Baruah et al., 2019). In the case of homogeneous photocatalysis (in the $nTiO_2$ treatments), $nTiO_2$ is well distributed in the water phase so that hydroxyl radicals are also generated throughout the entire test vessel. In contrast, in the case of heterogeneous photocatalysis, the $nTiO_2$ adsorbed on floating MPs (in the $nTiO_2$-loaded MPs treatments) generated hydroxyl radicals only locally, that is near the water surface. The latter assumption is supported by the fact that hydroxyl radicals are relatively short-lived and they travel only a limited distance from their source (Kehrer et al., 2010). This agrees well with the results of the ecotoxicity tests. After 12 h, *Daphnia* immobility was comparable between MPs and $nTiO_2$-loaded MPs, while $nTiO_2$ alone resulted in much higher effects at concentrations comparable to those applied in the $nTiO_2$-loaded MPs treatment. Since *Daphnia* actively avoid UV radiation (Rhode et al., 2001) they hid at the bottom of the vessel (in all UV treatments; Fig. 5B). By doing so, *Daphnia* were likely protected from the

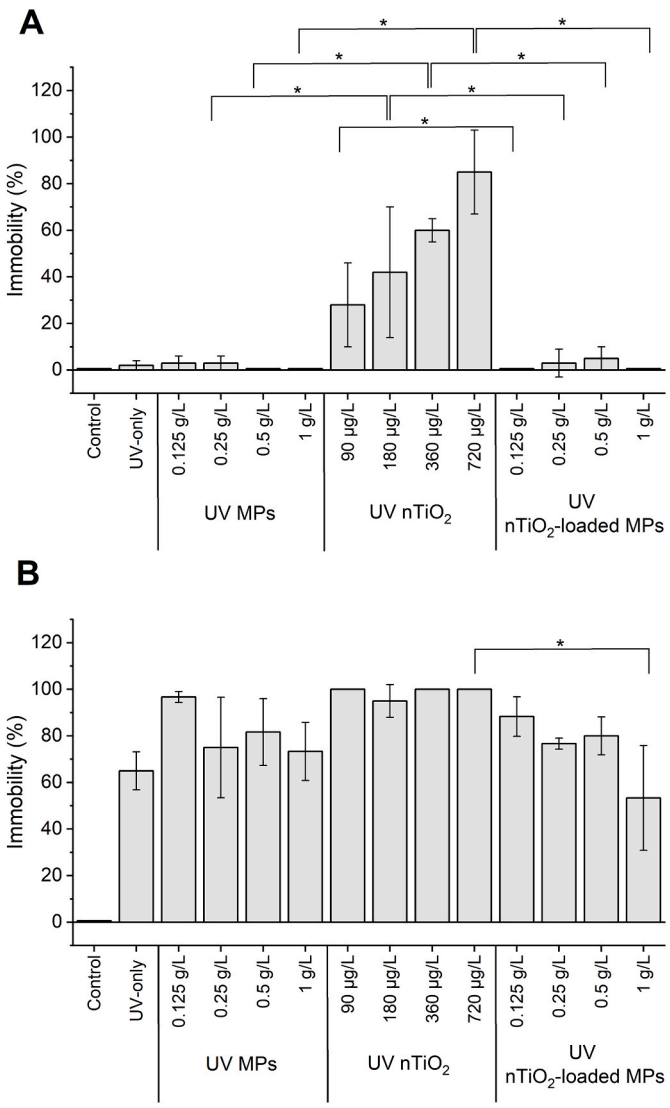


**Fig. 4.** Immobility of *Daphnia* (mean ± SD; n = 3) in the control, in the sole presence of UV light (UV-only) and when UV light is combined with MPs (c = 0.125, 0.25, 0.5, 1 g/L), $nTiO_2$ (c = 90, 180, 360, 720 µg/L), and $nTiO_2$-loaded MPs (c = 0.125, 0.25, 0.5, 1 g/L with adsorbed 90, 180, 360, 720 µg $nTiO_2$, respectively) after 12 (A) and 24 h (B). Asterisks denote significant differences between MPs, $nTiO_2$ and $nTiO_2$-loaded MPs treatments (Note that statistical significance was tested by including all outcomes; each treatment was replicated four times within an experiment, and the experiment was repeated three times, yielding n = 12). The difference between control and UV-only treatment and other treatments were also statistically tested but for the simplification of the figure the statistically significant difference was not denoted by asterisks.

hydroxyl radicals generated near the water surface where $nTiO_2$-loaded MPs floated, so the effect of hydroxyl radicals on *Daphnia* was negligible. In addition, suspended $nTiO_2$ can also coat the surface of organisms (Dabrunz et al., 2011) and it is thus plausible that hydroxyl radicals are also formed on the surface of organisms under UV irradiation, enhancing the deleterious effect of $nTiO_2$ on *Daphnia* after 12 h of exposure. After 24 h, immobility was comparable for all treatments, suggesting that prolonged UV irradiation has a major effect on immobility regardless of the presence of MPs or $nTiO_2$. In addition, the immobility of *Daphna* slightly decreased with increasing concentration of MPs and $nTiO_2$--loaded MPs in the test. This may be attributed to the absorption of UV radiation by floating MPs, as PE has an absorption spectrum in the UV wavelength range (Kuria Kamweru et al., 2014; Aji et al., 2018). In other words, a higher number of MPs and $nTiO_2$-loaded MPs floating on the surface means that larger surfaces scavenge UV light before it reaches *Daphnia* in the test system and consequently reduce UV-induced toxicity.

It is important to note that, in the absence of UV light, *Daphnia* were not affected by MPs, $nTiO_2$ nor $nTiO_2$-loaded MPs. This was expected because MPs were made of PE with a low density, most of them floated on the water surface and were therefore not available to *Daphnia.* However, when MPs come into contact with organisms at the water surface, such as floating plants, they may be adsorbed and cause mechanical damage to the tissue due to their abrasiveness (Kalčíková et al., 2017b, 2020). Also, $nTiO_2$ did not affect *Daphnia* mobility during 24 h, which is consistent with a large body of literature reporting no or limited acute ecotoxicity of $nTiO_2$ in the absence of UV light over this short exposure period (Heinlaan et al., 2008; Dalai et al., 2013; Seitz et al., 2015).

## 5. Conclusion

In summary, $nTiO_2$ were rapidly adsorbed on the surface of MPs and were evenly distributed on the MPs surface. The desorption of $nTiO_2$ from the surface of MPs into the medium was negligible, confirming the strong binding of $nTiO_2$ to the surface of MPs facilitating co-transport of both particles. Both suspended and adsorbed $nTiO_2$ showed photocatalytic properties and under UV irradiation a comparable amount of hydroxyl radicals was generated. However, the adsorbed $nTiO_2$ generated hydroxyl radicals only locally near the water surface, so that *Daphnia* hiding at the bottom of the vessel were not affected as much as in the presence of suspended $nTiO_2$. Nonetheless, aquatic organisms which are associated with the water surface at some point during their life cycle (e.g., phytoplankton, emerging insect, floating plants) could still be substantially affected as the formation of hydroxyl radicals appears to be concentrated in that environmental compartment. As field relevant levels of both MPs and NPs are an order of magnitude below those selected for this study and the UV conditions are more complex in the field, the environmental relevance of those insights need further attention. Since the interactions of MPs and metal NPs – widespread anthropogenic pollutants – still represent a significant data gap, a systematic assessment of their joint long-term effects under environmentally relevant conditions with more realistic concentrations is recommended.

## Credit author statement

**Gabriela Kalčíková**: Conceptualization, Methodology, Investigation, Writing – original draft, Writing - Review & Editing, Supervision, Funding acquisition, Resources, **Rajdeep Roy**: Investigation, Methodology, **Barbara Klun**: Investigation, **Ula Rozman**: Investigation, Methodology, Writing – original draft, Visualization, Writing - Review & Editing, **Gregor Marolt**: Investigation, **Tina Skalar**: Investigation, **Alexander Feckler**: Investigation, Methodology, **Mirco Bundschuh**: Conceptualization, Writing – original draft, Writing - Review & Editing, Supervision, Funding acquisition, Resources.

## Declaration of competing interest

The authors declare that they have no known competing financial interests or personal relationships that could have appeared to influence the work reported in this paper.

## Data availability

Data will be made available on request.

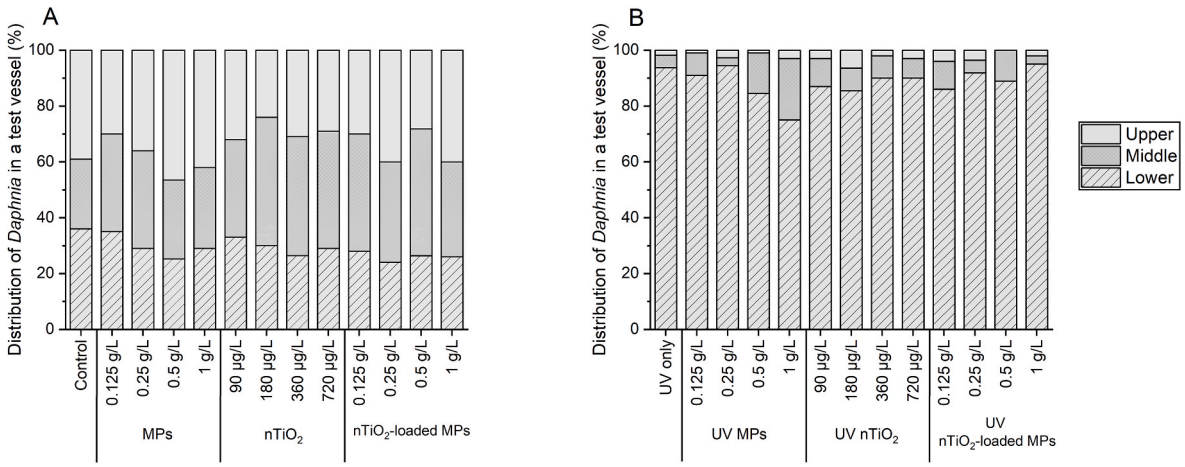


**Fig. 5.** Distribution of *Daphnia* in test vessels (upper, middle, and lower third of the water column) during the first 11 h of the experiment (mean; n = 22) in the absence (A) and in the presence (B) of UV light.


## Acknowledgement

The work was financed by the Slovenian Research Agency (Research programmes Chemical Engineering (P2-0191), Research and Development of Analytical Methods and Procedures (P1-0153) and Advanced Inorganic Chemistry (P1-0175), projects *PLAStouch* N2-0298 and *Plasti-C-Wetland* J2-2491 (https://planterastics.fkkt.uni-lj.si/)) and by German Academic Exchange Service (Grant No. 57299294) and it was also supported by the Centre for Research Infrastructure (Unit for analysis of small molecules), Faculty of Chemistry and Chemical Technology, University of Ljubljana. This publication is based upon work from COST Action CA20101 Plastics monitoRIng detectiOn RemedIaTion recoverY - PRIORITY, supported by COST (European Cooperation in Science and Technology, www.cost.eu).


## Appendix A. Supplementary data

Supplementary data to this article can be found online at https://doi.org/10.1016/j.chemosphere.2023.138628.

## References


Acosta-Coley, I., Mendez-Cuadro, D., Rodriguez-Cavallo, E., de la Rosa, J., Olivero-Verbel, J., 2019. Trace elements in microplastics in Cartagena: a hotspot for plastic pollution at the Caribbean. Mar. Pollut. Bull. 139, 402–411.

Aji, M.P., Rahmawati, I., Priyanto, A., Karunawan, J., Wati, A.L., Aryani, N.P., Susanto Wibowo, E., Sulhadi, 2018. Optical absorption in recycled waste plastic polyethylene. J. Phys. Conf. 983, 012007.

ASTM, 2007. Standard Guide for Conducting Acute Toxicity Tests on Test Material with Fishes, Macroinvertebrates, and Amphibians. ASTM International, West Conshocken, pp. 1–22.

Atugoda, T., Vithanage, M., Wijesekara, H., Bolan, N., Sarmah, A.K., Bank, M.S., You, S., Ok, Y.S., 2021. Interactions between microplastics, pharmaceuticals and personal care products: implications for vector transport. Environ. Int. 149, 106367.

Baruah, A., Chaudhary, V., Malik, R., Tomer, V.K., 2019. 17 - nanotechnology based solutions for wastewater treatment. In: Ahsan, A., Ismail, A.F. (Eds.), Nanotechnology in Water and Wastewater Treatment. Elsevier, pp. 337–368.

Binda, G., Spanu, D., Monticelli, D., Pozzi, A., Bellasi, A., Bettinetti, R., Carnati, S., Nizzetto, L., 2021. Unfolding the interaction between microplastics and (trace) elements in water: a critical review. Water Res. 204, 117637.

Borgmann, U., 1996. Systematic analysis of aqueous ion requirements of Hyalella azteca: a standard artificial medium including the essential bromide ion. Arch. Environ. Contam. Toxicol. 30, 356–363.

Bundschuh, M., Zubrod, J.P., Englert, D., Seitz, F., Rosenfeldt, R.R., Schulz, R., 2011. Effects of nano-TiO2 in combination with ambient UV-irradiation on a leaf shredding amphipod. Chemosphere 85, 1563–1567.

Burns, E.E., Boxall, A.B.A., 2018. Microplastics in the aquatic environment: evidence for or against adverse impacts and major knowledge gaps. Environ. Toxicol. Chem. 37, 2776–2796.

Cai, L., He, L., Peng, S., Li, M., Tong, M., 2019. Influence of titanium dioxide nanoparticles on the transport and deposition of microplastics in quartz sand. Environ. Pollut. 253, 351–357.

Cao, Y., Zhao, M., Ma, X., Song, Y., Zuo, S., Li, H., Deng, W., 2021. A critical review on the interactions of microplastics with heavy metals: mechanism and their combined effect on organisms and humans. Sci. Total Environ. 788, 147620.

Chibowski, S., Paszkiewicz, M., 2001. Studies of some properties and the structure of polyethylene glycol (PEG) macromolecules adsorbed on a TiO2 surface. Adsorpt. Sci. Technol. 19, 397–407.

Choi, S.K., 2016. Mechanistic basis of light induced cytotoxicity of photoactive nanomaterials. NanoImpact 3–4, 81–89.

Cypriyana, P.J.J., S, S., Angalene J, L.A., Samrot, A.V., Kumar S, S., Ponniah, P., Chakravarthi, S., 2021. Overview on toxicity of nanoparticles, it's mechanism, models used in toxicity studies and disposal methods – a review. Biocatal. Agric. Biotechnol. 36, 102117.

Dabrunz, A., Duester, L., Prasse, C., Seitz, F., Rosenfeldt, R., Schilde, C., Schaumann, G. E., Schulz, R., 2011. Biological surface coating and molting inhibition as mechanisms of TiO2 nanoparticle toxicity in Daphnia magna. PLoS One 6, e20112.

Dalai, S., Pakrashi, S., Chandrasekaran, N., Mukherjee, A., 2013. Acute toxicity of TiO2 nanoparticles to Ceriodaphnia dubia under visible light and dark conditions in a freshwater system. PLoS One 8, e62970.

Das, R.K., Sanyal, D., Kumar, P., Pulicharla, R., Brar, S.K., 2021. Science-society-policy interface for microplastic and nanoplastic: environmental and biomedical aspects. Environ. Pollut. 290, 117985.

Davarpanah, E., Guilhermino, L., 2019. Are gold nanoparticles and microplastics mixtures more toxic to the marine microalgae Tetraselmis chuii than the substances individually? Ecotoxicol. Environ. Saf. 181, 60–68.

De Falco, F., Di Pace, E., Cocca, M., Avella, M., 2019. The contribution of washing processes of synthetic clothes to microplastic pollution. Sci. Rep. 9, 6633.

Feckler, A., Rosenfeldt, R.R., Seitz, F., Schulz, R., Bundschuh, M., 2015. Photocatalytic properties of titanium dioxide nanoparticles affect habitat selection of and food quality for a key species in the leaf litter decomposition process. Environ. Pollut. 196, 276–283.

Ferreira, P., Fonte, E., Soares, M.E., Carvalho, F., Guilhermino, L., 2016. Effects of multi-stressors on juveniles of the marine fish Pomatoschistus microps: gold nanoparticles, microplastics and temperature. Aquat. Toxicol. 170, 89–103.

Fu, L., Li, J., Wang, G., Luan, Y., Dai, W., 2021. Adsorption behavior of organic pollutants on microplastics. Ecotoxicol. Environ. Saf. 217, 112207.

Godoy, V., Martín-Lara, M.A., Calero, M., Blázquez, G., 2019. Physical-chemical characterization of microplastics present in some exfoliating products from Spain. Mar. Pollut. Bull. 139, 91–99.

Hahladakis, J.N., Velis, C.A., Weber, R., Iacovidou, E., Purnell, P., 2018. An overview of chemical additives present in plastics: migration, release, fate and environmental impact during their use, disposal and recycling. J. Hazard Mater. 344, 179–199.

Hartmann, N.B., Hüffer, T., Thompson, R.C., Hassellöv, M., Verschoor, A., Daugaard, A. E., Rist, S., Karlsson, T., Brennholt, N., Cole, M., Herrling, M.P., Hess, M.C., Ivleva, N. P., Lusher, A.L., Wagner, M., 2019. Are we speaking the same language? Recommendations for a definition and categorization framework for plastic debris. Environ. Sci. Technol. 53, 1039–1047.

Heinlaan, M., Ivask, A., Blinova, I., Dubourguier, H.-C., Kahru, A., 2008. Toxicity of nanosized and bulk ZnO, CuO and TiO2 to bacteria Vibrio fischeri and crustaceans Daphnia magna and Thamnocephalus platyurus. Chemosphere 71, 1308–1316.

Ho, Y.S., McKay, G., 1999. Pseudo-second order model for sorption processes. Process Biochem. 34, 451–465.

Horton, A.A., Svendsen, C., Williams, R.J., Spurgeon, D.J., Lahive, E., 2017. Large microplastic particles in sediments of tributaries of the River Thames, UK – abundance, sources and methods for effective quantification. Mar. Pollut. Bull. 114, 218–226.

Kalčíková, G., Alič, B., Skalar, T., Bundschuh, M., Gotvajn, A.Ž., 2017a. Wastewater treatment plant effluents as source of cosmetic polyethylene microbeads to freshwater. Chemosphere 188, 25–31.

Kalčíková, G., Englert, D., Rosenfeldt, R.R., Seitz, F., Schulz, R., Bundschuh, M., 2014. Combined effect of UV-irradiation and TiO2-nanoparticles on the predator–prey interaction of gammarids and mayfly nymphs. Environ. Pollut. 186, 136–140.
Kalčíková, G., Skalar, T., Marolt, G., Jemec Kokalj, A., 2020. An environmental concentration of aged microplastics with adsorbed silver significantly affects aquatic organisms. Water Res. 175, 115644.
Kalčíková, G., Žgajnar Gotvajn, A., Kladnik, A., Jemec, A., 2017b. Impact of polyethylene microbeads on the floating freshwater plant duckweed Lemna minor. Environ. Pollut. 230, 1108–1115.
Kehrer, J.P., Robertson, J.D., Smith, C.V., 2010. 1.14 - free radicals and reactive oxygen species. In: McQueen, C.A. (Ed.), Comprehensive Toxicology, second ed. Elsevier, Oxford, pp. 277–307.
Kuria Kamweru, P., Gichuki Ndiritu, F., Kinyanjui, T., Wanjiku Muthui, Z., Gichuki Ngumbu, R., Migunde Odhiambo, P., 2014. UV absorption and dynamic mechanical analysis of polyethylene films. Int. J. Phys. Sci. 9, 545–555.
Lagergren, S., 1898. About the theory of so-called adsorption of soluble substances. KUNGLIGA SVENSKA VETENSKAPSAKADEMIENS HANDLINGAR 24, 1–39.
Li, P., Zou, X., Wang, X., Su, M., Chen, C., Sun, X., Zhang, H., 2020. A preliminary study of the interactions between microplastics and citrate-coated silver nanoparticles in aquatic environments. J. Hazard Mater. 385, 121601.
Liu, W., Zhang, J., Liu, H., Guo, X., Zhang, X., Yao, X., Cao, Z., Zhang, T., 2021. A review of the removal of microplastics in global wastewater treatment plants: characteristics and mechanisms. Environ. Int. 146, 106277.
Luo, H., Xiang, Y., Li, Y., Zhao, Y., Pan, X., 2020. Weathering alters surface characteristic of TiO2-pigmented microplastics and particle size distribution of TiO2 released into water. Sci. Total Environ. 729, 139083.
Lüderwald, S., Dackermann, V., Seitz, F., Adams, E., Feckler, A., Schilde, C., Schulz, R., Bundschuh, M., 2019. A blessing in disguise? Natural organic matter reduces the UV light-induced toxicity of nanoparticulate titanium dioxide. Sci. Total Environ. 663, 518–526.
Ma, H., Pu, S., Liu, S., Bai, Y., Mandal, S., Xing, B., 2020. Microplastics in aquatic environments: toxicity to trigger ecological consequences. Environ. Pollut. 261, 114089.
Mai, L., Bao, L.-J., Shi, L., Liu, L.-Y., Zeng, E.Y., 2018. Polycyclic aromatic hydrocarbons affiliated with microplastics in surface waters of Bohai and Huanghai Seas, China. Environ. Pollut. 241, 834–840.
Malakar, A., Kanel, S.R., Ray, C., Snow, D.D., Nadagouda, M.N., 2021. Nanomaterials in the environment, human exposure pathway, and health effects: a review. Sci. Total Environ. 759, 143470.
Napper, I.E., Bakir, A., Rowland, S.J., Thompson, R.C., 2015. Characterisation, quantity and sorptive properties of microplastics extracted from cosmetics. Mar. Pollut. Bull. 99, 178–185.
OECD, 2004. Test No. 202: Daphnia Sp. Acute Immobilisation Test. OECD Guideline for Testing of Chemicals. OECD Publishing, Paris, pp. 1–12.
Pacheco, A., Martins, A., Guilhermino, L., 2018. Toxicological interactions induced by chronic exposure to gold nanoparticles and microplastics mixtures in Daphnia magna. Sci. Total Environ. 628–629, 474–483.
Park, C.M., Chu, K.H., Her, N., Jang, M., Baalousha, M., Heo, J., Yoon, Y., 2017. Occurrence and removal of engineered nanoparticles in drinking water treatment and wastewater treatment processes. Separ. Purif. Rev. 46, 255–272.
Patchaiyappan, A., Dowarah, K., Zaki Ahmed, S., Prabakaran, M., Jayakumar, S., Thirunavukkarasu, C., Devipriya, S.P., 2021. Prevalence and characteristics of microplastics present in the street dust collected from Chennai metropolitan city, India. Chemosphere 269, 128757.
R Core Team, 2020. R: A Language and Environment for Statistical Computing. R Foundation for Statistical Computing, Vienna, Austria.
Rezania, S., Park, J., Md Din, M.F., Mat Taib, S., Talaiekhozani, A., Kumar Yadav, K., Kamyab, H., 2018. Microplastics pollution in different aquatic environments and biota: a review of recent studies. Mar. Pollut. Bull. 133, 191–208.
Rhode, S.C., Pawlowski, M., Tollrian, R., 2001. The impact of ultraviolet radiation on the vertical distribution of zooplankton of the genus Daphnia. Nature 412, 69–72.
Rozman, U., Turk, T., Skalar, T., Zupančič, M., Čelan Korošin, N., Marinšek, M., Olivero-Verbel, J., Kalčíková, G., 2021. An extensive characterization of various environmentally relevant microplastics – material properties, leaching and ecotoxicity testing. Sci. Total Environ. 773, 145576.
Sahoo, T.R., Prelot, B., 2020. Chapter 7 - adsorption processes for the removal of contaminants from wastewater: the perspective role of nanomaterials and nanotechnology. In: Bonelli, B., Freyria, F.S., Rossetti, I., Sethi, R. (Eds.), Nanomaterials for the Detection and Removal of Wastewater Pollutants. Elsevier, pp. 161–222.
Seitz, F., Bundschuh, M., Rosenfeldt, R.R., Schulz, R., 2013. Nanoparticle toxicity in Daphnia magna reproduction studies: the importance of test design. Aquat. Toxicol. 126, 163–168.
Seitz, F., Lüderwald, S., Rosenfeldt, R.R., Schulz, R., Bundschuh, M., 2015. Aging of TiO2 nanoparticles transiently increases their toxicity to the pelagic microcrustacean Daphnia magna. PLoS One 10, e0126021.
Tang, B., Zhang, L., Geng, Y., 2005. Determination of the antioxidant capacity of different food natural products with a new developed flow injection spectrofluorimetry detecting hydroxyl radicals. Talanta 65, 769–775.
Venables, W.N., Ripley, B.D., 2002. Modern Applied Statistics with S, fourth ed. Springer, New York.
Wang, J., Guo, X., 2020. Adsorption kinetic models: physical meanings, applications, and solving methods. J. Hazard Mater. 390, 122156.
Yu, F., Yang, C., Zhu, Z., Bai, X., Ma, J., 2019. Adsorption behavior of organic pollutants and metals on micro/nanoplastics in the aquatic environment. Sci. Total Environ. 694, 133643.
Zhang, J., Nosaka, Y., 2014. Mechanism of the OH radical generation in photocatalysis with TiO2 of different crystalline types. J. Phys. Chem. C 118, 10824–10832.